Frequency trends of acoustic radiation modes for cylindrical structures

Caleb B. Goates, Scott D. Sommerfeldt, and Jonathan D. Blotter

---

ARTICLES YOU MAY BE INTERESTED IN

A quasi-analytical formulation for acoustic radiation modes of simple curved structures
The Journal of the Acoustical Society of America **144**, 1862 (2018); https://doi.org/10.1121/1.5068189

Sound radiation and transonic boundaries of a plate with an acoustic black hole
The Journal of the Acoustical Society of America **145**, 164 (2019); https://doi.org/10.1121/1.5081680

On the physical meaning of subsonic wavenumber truncation as applied to source identification on vibrating structures
Proceedings of Meetings on Acoustics **35**, 065001 (2018); https://doi.org/10.1121/2.0000964

How POMA and other conference proceedings empower students to publish
Proceedings of Meetings on Acoustics **36**, 032001 (2019); https://doi.org/10.1121/2.0001001

Computation of dispersion curves of guided waves in functionally graded materials
Proceedings of Meetings on Acoustics **33**, 045002 (2018); https://doi.org/10.1121/2.0001014

A method for locating acoustic emission events using amplitude stacking weighted waveform correlation
Proceedings of Meetings on Acoustics **36**, 055001 (2019); https://doi.org/10.1121/2.0001017

Structural Acoustics and Vibration: Paper 3pSA4

Frequency trends of acoustic radiation modes for cylindrical structures

Caleb B. Goates and Scott D. Sommerfeldt
Department of Physics and Astronomy, Brigham Young University, Provo, UT, 84602;
calebgoates@gmail.com; scott_sommerfeldt@byu.edu;

Jonathan D. Blotter
Department of Mechanical Engineering, Brigham Young University, Provo, UT, 84602; jblotter@byu.edu

    Acoustic radiation modes have become a useful and widespread analysis tool in situations involving sound radiation from vibrating structures. They have found use in applications such as active structural acoustic control, optimization of structures for minimal sound radiation, and acoustical holography. Analytical expressions for the radiation resistance matrix, from which the radiation modes are obtained, are available only for a small number of simple source geometries, while the obtaining of radiation modes for more complicated structures typically requires boundary element analysis or similar computational methods. In addition, better characterization of radiation modes could lead to rules of thumb or expressions for evaluating them more quickly, e.g. when the modes must be evaluated across a wide frequency band. This paper details the development of quasi-analytical expressions for the radiation resistance matrices of singly-curved structures such as cylinders, cylindrically curved plates, and angularly truncated cylinders. Through these expressions, radiation modes for these structures may be obtained without the use of typical computational methods. Wavenumber transforms of these modes are shown, and trends of the physical and wavenumber space representations are investigated as frequency varies. It is found that the most efficient modes morph with frequency to match the acoustic wavenumber.

1. INTRODUCTION

Acoustic radiation modes form an orthogonal basis that describes the radiation of sound from a surface velocity distribution. These modes have long been present in the search for a meaningful connection between vibration patterns and the resulting acoustic radiation, but they are less often utilized than the more popular methods of wavenumber filtering and structural-mode-based analysis. In contrast to structural modes, the radiation modes do not depend on the material or mounting conditions of the vibrating structure, but only on the geometry of the fluid-structure interface. They also orthogonalize the radiation operator, meaning that they radiate sound power independently of one another, while structural modes exhibit coupling in the generation of sound power. Radiation modes originally found use in active structural acoustic control as a metric for reducing total sound power;[1] because each radiation mode radiates sound power independently, minimizing vibration in one radiation mode invariably lowers the total sound power radiated. More recently, radiation modes have been investigated as a method of calculating sound power from experimental vibration measurements,[2] as basis functions for acoustical holography,[3] and as design parameters for quieter structures.[4]

Though not originally known by their current name, radiation modes were first introduced in the literature in the early 1990s through three papers published within a year of each other. Photaidis first published a paper on the relationship between radiation modes and wavenumber filtering,[5] though he cited Borgiotti as the first to employ the modes. Borgiotti's paper came two months later, focusing on the relationships between radiation modes and the radiated sound power.[6] The third paper, by Sarkissian, introduced a simpler way to calculate radiation modes by eigenvector decomposition of the radiation resistance matrix;[7] this is the method commonly used today. Both Sarkissian and Photaidis were clear that radiation modes tend to have a preferential or peak wavenumber and that at high enough acoustic wavenumber k, the radiation modes with peak wavenumbers nearest to k tended to be the most efficient radiators of power. This was shown by examples at various frequencies.

At the present state of the literature, analytical formulations for the acoustic radiation modes, or the radiation resistance matrix from which they are derived, exist for two structure-fluid interface geometries, namely flat plates in infinite baffles and spheres. All other modes must be calculated through the means of boundary integral equations or the boundary element method, as described in Ref. 3. This requires significantly more computational power than the simple evaluation of expressions for the modes, especially if modes are needed over a large frequency range. Computational demands of radiation mode calculations could be minimized through additional analytical expressions for modes, as well as through better characterization of mode trends over frequency. Efforts in this latter regard have recently been undertaken for sphero-cubic structures,[8] and the current work attempts to further develop such characterizations.

This paper presents a formulation for the radiation resistance matrix of cylindrically curved objects. The matrix is formulated in terms of the cylindrical eigenfunctions of the wave equation. The resulting radiation modes are presented along with insight into their trends with frequency. Not only are the features noted by Photaidis and Sarkissian observed again here, but the trends of these features as the frequency is varied are investigated. It is found that the modes morph to meet the requirement that the most efficient modes must have peak wavenumber close to k. In addition, Sarkissian and Photaidis investigated only the axial dependence of radiation modes with axial symmetry, but here the full two-dimensional cylinder modes are shown, and the effects of the azimuthal dependence is shown in both wavenumber and physical domains.

2. METHODS

The radiation resistance matrix is derived from the expression for sound power radiated from a vibrating structure. Given the acoustic pressure $\tilde{p}$ and the normal structure velocity $\tilde{u}$, the sound power may be calculated as

$$\Pi = \frac{1}{2}\operatorname{Re}\left\{\int_S \tilde{p}^*\tilde{u}\,dS\right\}, \tag{1}$$

where S is the surface of the vibrating structure, and $(\cdot)^*$ denotes the complex conjugate. If the vibrating structure is discretized into N discrete radiators of equal area, this may be rewritten in vector form as

$$\Pi = \frac{S}{2N}\operatorname{Re}\{\vec{p}^H\vec{u}\} \tag{2}$$

where $\vec{p}$ and $\vec{u}$ are $1 \times N$ vectors containing the acoustic pressure and normal surface velocity, respectively, evaluated at each surface point, and $(\cdot)^H$ indicates the Hermitian transpose. Because the pressure can be written in terms of the surface velocity through Green's functions, it is possible to write the power in terms of the surface velocities only as

$$\Pi = \frac{S}{2N}\operatorname{Re}\{\vec{u}^H \mathbf{Z}\vec{u}\} = \frac{S}{2N}\vec{u}^H\operatorname{Re}\{\mathbf{Z}\}\vec{u}, \tag{3}$$

where $\mathbf{Z}$ is the matrix of Green's functions between each pair of locations. The radiation resistance matrix is then defined as

$$\mathbf{R} = \frac{S_e}{2}\operatorname{Re}\{\mathbf{Z}\}, \tag{4}$$

with $S_e = S/N$ being the area of a single discrete radiator. Therefore, the derivation of the radiation resistance matrix is as simple as finding the Green's function between surface points.

This paper presents eigenfunction decomposition formulations for the radiation resistance matrix of cylindrically curved objects in separable geometries. These geometries, shown in Fig. 1, include a full cylinder of finite length on an infinite cylindrical baffle, as in Fig. 1(a); a partial cylinder on an infinite cylindrical baffle, as shown in Fig. 1(b); and a partial cylinder radiating into a partial cylindrical space of extent θ_L, as shown in Fig 1(c). In each of these figures, grey surfaces are presumed to continue out to infinity.

a)   b)   c)
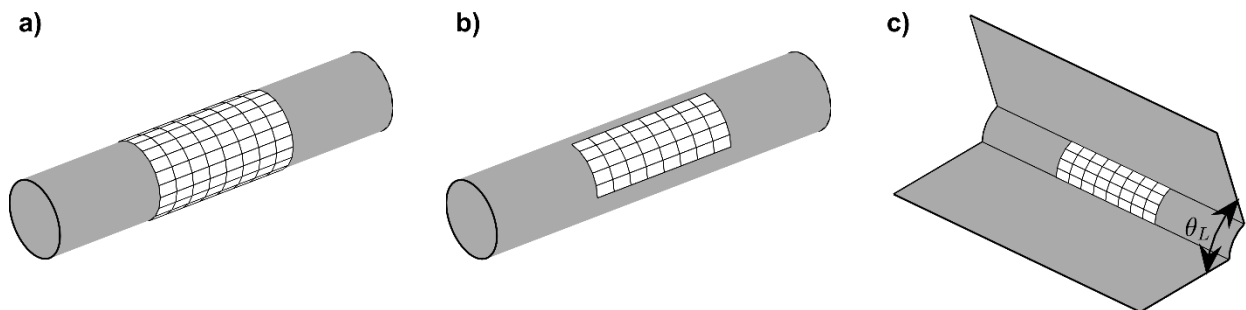

Figure 1: Cylindrical structures treated in this work. (a) A finite cylinder on an infinite cylindrical baffle. (b) A partial cylinder on an infinite cylindrical baffle. (c) A partial cylinder radiating into a partial cylindrical space of θ-extent θ_L.

The derivation is as follows: The eigenfunction decomposition in cylindrical coordinates allows the pressure field generated by the vibration of one discrete element to be expressed in the form

$$p(r, \theta, z) = \sum_{m=0}^{\infty} \int_0^{\infty} dk_z \, (A_m \cos m\theta + B_m \sin m\theta)$$
$$\times \, (D(k_z) \cos k_z z + E(k_z) \sin k_z z) H_m^{(2)}(k_r r) \tag{5}$$

where m and k_z are separation constants, $k_r = \sqrt{k^2 - k_z^2}$, and $A_m, B_m, D(k_z)$, and $E(k_z)$ are constants to be determined. The velocity when one discrete element of the structure is vibrating may be approximated with a point source of equivalent source strength. Then, expanding the point source in terms of the θ and z eigenfunctions, and applying Euler's equation at the surface of the structure, we can find that the ijth element of the radiation resistance matrix for the first two structures in Fig. 1 is

$$R_{ij} = \frac{\omega \rho_0 S_e^2}{a\pi^2} \sum_{m=0}^{\infty} \cos(m\Delta\theta_{ij}) \int_0^k \mathrm{Im} \left\{ \frac{H_m^{(2)}(k_r a)}{k_r H_m^{(2)\prime}(k_r a)} \right\} \cos(k_z \Delta z_{ij}) \, dk_z, \tag{6}$$

where a is the radius of the cylinder, ω is the angular frequency, ρ_0 is the density of air, and $\Delta\theta_{ij}$ and Δz_{ij} are the difference in θ position and z position of the ith and jth discrete elements. For the structure in Fig. 1(c) there are homogeneous Neumann boundary conditions at $\theta = 0, \theta_L$ instead of a periodicity condition. Thus the finished expression is

$$R_{ij} = \frac{\omega \rho_0 S_e^2}{\pi a \theta_L} \sum_{m=0}^{\infty} \cos\left(\frac{m\pi\theta_i}{\theta_L}\right) \cos\left(\frac{m\pi\theta_j}{\theta_L}\right) \int_0^k \mathrm{Im} \left\{ \frac{H_{m\pi/\theta_L}^{(2)}(k_r a)}{k_r H_{m\pi/\theta_L}^{(2)\prime}(k_r a)} \right\} \cos(k_z \Delta z_{ij}) \, dk_z, \tag{7}$$

where θ_i and θ_j are the θ positions of the ith and jth discrete elements.

The radiation resistance matrices in Eqs. (6) and (7) may be used for power calculations as in Eq. (3), or they may be decomposed into the radiation modes. Eigendecomposition of these matrices gives eigenvectors $\{q_r\}$, which are the radiation modes, and eigenvalues $\{\lambda_r\}$, which are proportional to the radiation efficiencies of the associated modes. The radiation modes are presented in the following section at various kL values for a cylinder with $L/a = 6$ and with a θ extent of $\pi/2$ for the partial cylinders.

In addition to simply looking at the radiation modes themselves, the following results include wavenumber transforms of the radiation modes for a full cylinder. Because the radiation modes are real, the magnitude of the wavenumber transforms will be symmetrical across the axes; thus only the first quadrant of the wavenumber domain is shown. The radiation modes are padded by many zeros above and below the mode in the z direction to represent the rigid baffle, after which a two-dimensional fast Fourier transform is used. These transforms allow us to look for the trends that Sarkissian and Photaidis mentioned as the frequency varies.

3. RESULTS

The first nine radiation modes for each geometry are shown in Fig. 2 for $kL \ll 1$, sorted by radiation efficiency, with parts (a)-(c) corresponding to the geometries presented in Fig. 1, parts (a)-(c). For each geometry, there is a multipole-like pattern in the series of modes: The first mode is a breathing, or monopole mode, the next two or three modes feature two out of phase regions like a dipole, the few after that resemble longitudinal or lateral quadrupoles, and so on. This similarity can also be seen in a plot of the efficiencies, given for the full cylinder modes in Fig. 3; below about $kL = 0.5$ rad the monopolar modes follow a 6 dB/octave increase, the dipolar modes follow a 12 dB/octave trend, and the quadrupolar modes increase at 18 dB/octave. It is interesting to note that the mode shapes for the partial cylinders on a cylindrical baffle and those for partial cylinders radiating into a partial space are very similar at this low kL. Some of the modes switch places in the lineup of efficiency, and there are slight differences in those that match, but the general shapes are the same.
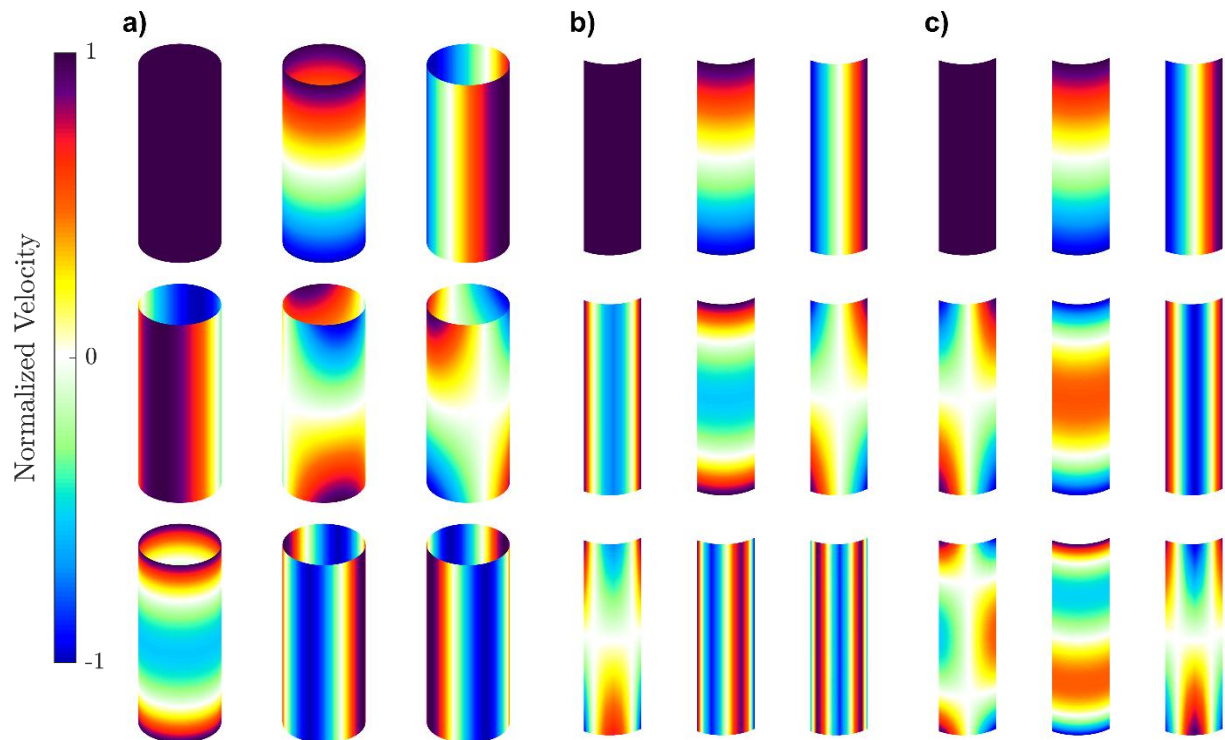
Figure 2: The nine most efficient acoustic radiation modes for each of the three geometries in Fig. 1. (a) Full cylinders, (b) Partial cylinders on a cylindrical baffle, (c) partial cylinders radiating into a quarter space.
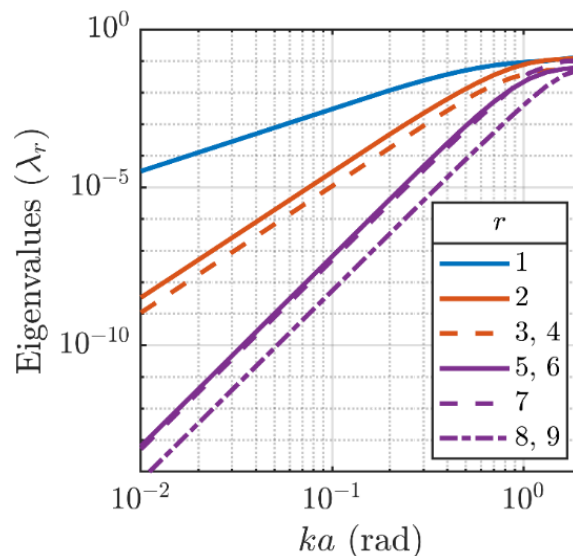

Figure 3: Efficiencies of the few most efficient full cylinder modes at low kL*. The multipole-like effects can be seen in the rate of increase of these efficiencies with frequency.*

Next we turn to the wavenumber transforms of the full cylinder modes. Initial wavenumber transforms of the most efficient modes with zero-order, first-order, and second-order θ dependence are shown in Fig. 4 for $kL = 6$. It is seen that each mode has only one wavenumber component in the θ

direction, corresponding to the order of the θ dependence. In other words, the θ dependence of each of the modes is purely sinusoidal. All wavenumber transforms for the balance of this paper will therefore be presented as line plots, showing the k_z dependence for only the k_θ value at which the transform is non-zero.
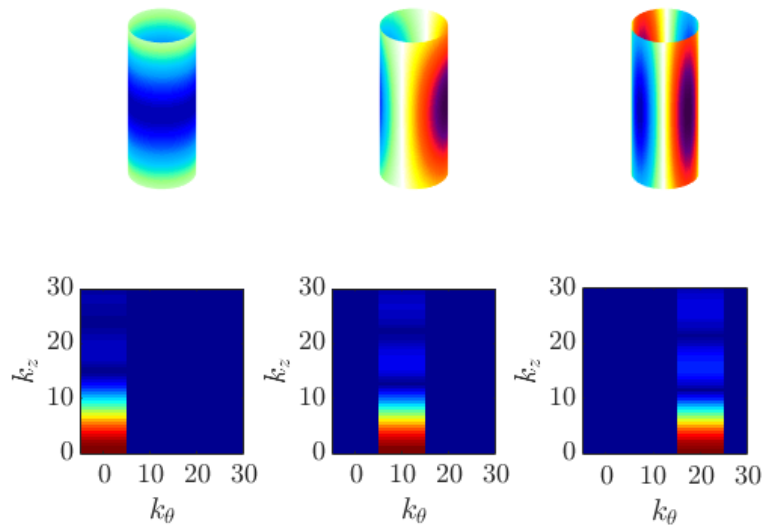

Figure 4: The most efficiently radiating modes with zero-order, first-order, and second-order θ dependence, and their associated 2D wavenumber transforms.

    These line plots are shown in Fig. 5 for the four most efficient modes (from left to right) with no θ dependence. Here we begin to look at trends with frequency, as the same four modes are shown at several kL values. In Fig. 5(a) the first four modes each peak at a different wavenumber, but as the acoustic wavenumber increases from $kL = 6$ to $kL = 9$ in Fig. 5(b), it is seen that the first two modes peak around the same $k_z L$, and the third mode has shifted to a peak wavenumber at $k_z L = 0$. As the frequency continues to increase, the first two modes peak at around the same wavenumber, which closely follows the acoustic wavenumber, and the third and fourth mode begin to peak at the same wavenumber as well, which follows after the more efficient modes' peak wavenumber. Animations of these trends, of which the plots in Fig. 5 are just a snapshot, can be found at https://doi.org/10.6084/m9.figshare.8248883.

    In other words, pairs of modes emerge that have the same or similar peak wavenumbers. The peak wavenumbers of the most efficient pair follow the acoustic wavenumber, and each subsequent pair of modes has a peak wavenumber that follows that of the pair before. In each pair of modes there is one mode which has even symmetry about the center of the structure's z-extent and one which has odd symmetry about that center. As the modes morph to higher wavenumbers, these symmetries do not change. It is interesting as well to look at the efficiencies of these pairs of modes at high kL. Shown in Fig. 6 are the efficiencies of the four modes whose trends are given in Fig. 5. It can be seen that at high enough kL the two modes with similar peak wavenumbers also have similar efficiencies. These efficiencies constantly leapfrog each other as the wavenumbers increase, but the pairs with no θ dependence do not overtake each other in efficiency. This means that the two most efficient modes will always be the two most efficient modes at high kL.
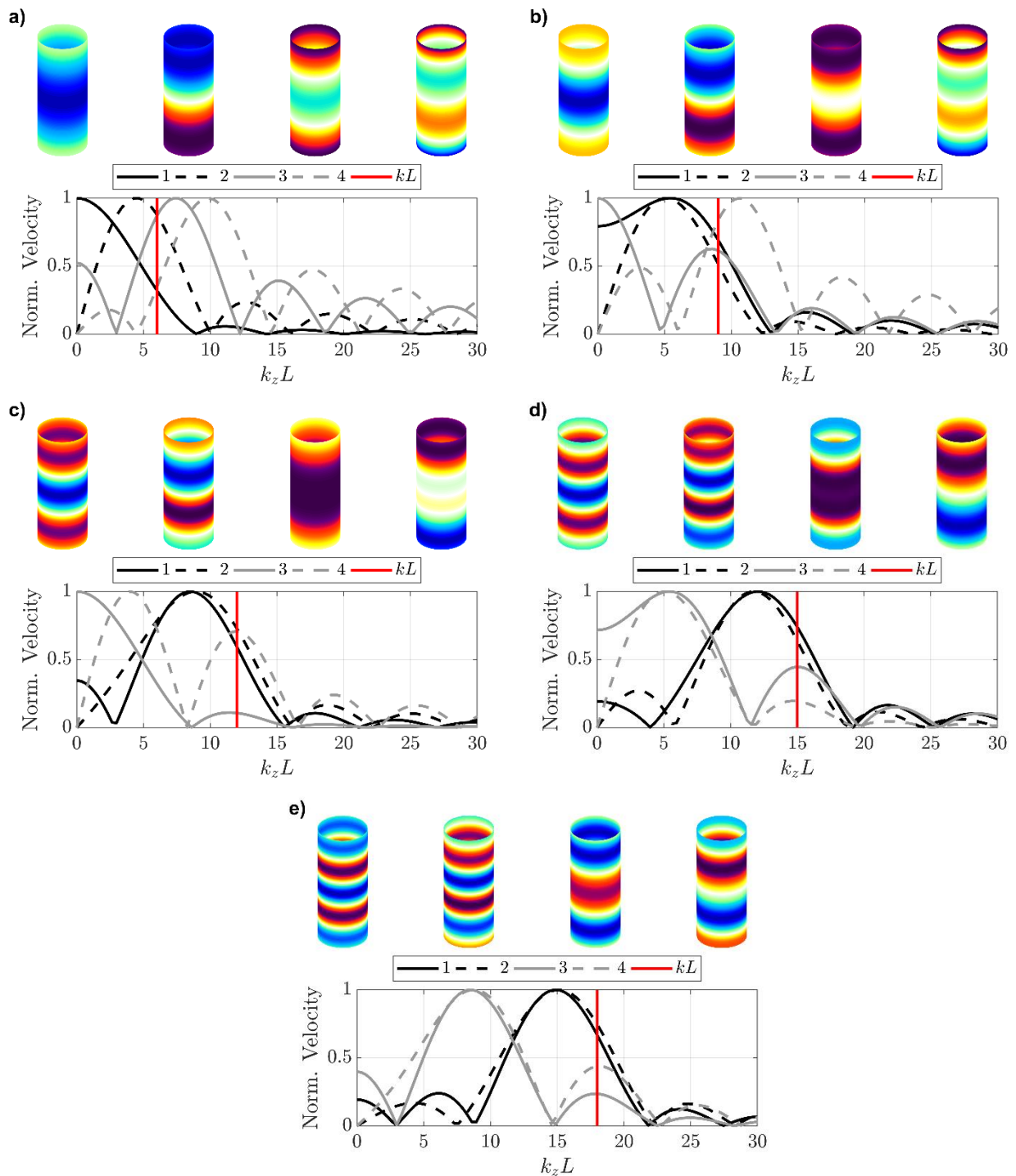
Figure 5: The physical space and wavenumber space representations of the first four radiation modes with no θ dependence. (a) at kL = 6. (b) at kL = 9. (c) at kL = 12. (d) at kL = 15. (e) at kL = 18.
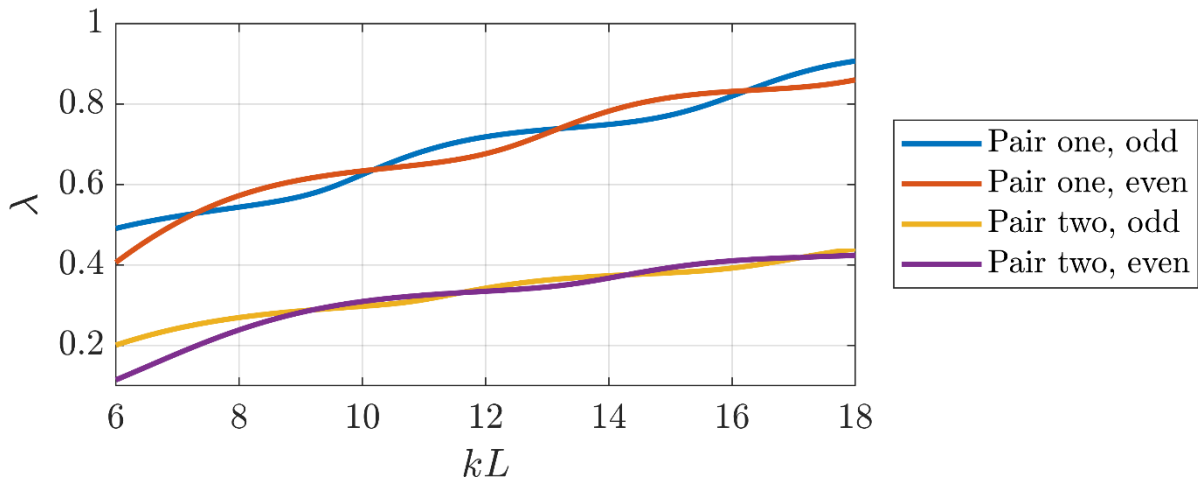
*Figure 6: Efficiency of the first few modes with zero-order and first-order θ dependence at high **kL***

The trends above are also exhibited in modes with first-order or second-order θ dependence, though with a slight variation. Figure 7 shows the four most efficient modes with second-order θ dependence at $kL = 18$, which corresponds to Fig. 5(e). These modes come in degenerate pairs; the first two modes have identical efficiencies and wavenumber transform magnitudes, as do the last two shown. The difference between the first and second (and between the third and fourth) modes is simply a $\sin 2\theta$ versus a $\cos 2\theta$ dependence. As such, all four of these modes become a peak wavenumber "pair" in which the peak wavenumbers are similar and change together with frequency. The wavenumber transforms shown here make obvious an important point; these most efficient modes with second-order θ dependence do not follow the acoustic wavenumber, but rather the effective acoustic wavenumber given by $\sqrt{k^2 - k_\theta^2}$, also known as the radiation circle. Animations of these modes and their wavenumber transforms as frequency is varied are also available at the link given above, https://doi.org/10.6084/m9.figshare.8248883.
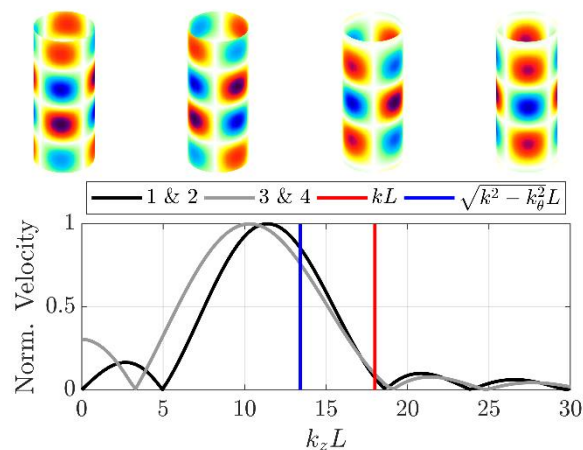

*Figure 7: The physical space and wavenumber space representations of the first four radiation modes with second-order θ dependence at **kL** = **18**.*

4. DISCUSSION

As has been shown above, the most efficient radiation modes have peak wavenumbers that tend to follow the radiation circle as it moves with frequency. This is true regardless of the circumferential wavenumber of the modes. While k_z changes with frequency in this case, k_θ does not. Similar analysis of the other structures given in Fig. 1 show that this morphing effect occurs in the z dimension for all three mode types, but in the θ dimension only for the partial cylinders on an infinite cylindrical baffle. Comparison with other known radiation modes, such as those for flat baffled plates and those for spheres, suggests that this morphing of radiation modes with frequency occurs only in dimensions where the structure does not span the whole dimensional space. For example, a vibrating sphere covers the whole ϕ and θ dimensions over which the fluid-structure interface is defined, and consequently there is no variation of the radiation modes with frequency. In contrast, the radiation modes of flat plates morph with frequency in both dimensions over which they are defined; this is because the flat plate does not cover the full breadth of either of those dimensions.

REFERENCES

[1] S. J. Elliot and M. E. Johnson, "Radiation modes and the active control of sound power," *J. Acoust. Soc. Am.* **94**(4) 2194-2204 (1993).

[2] M.R. Bai, M. Tsao, "Estimation of sound power of baffled planar sources using radiation matrices," *J. Acoust. Soc. Am* **112**, 876-883 (2002).

[3] J. Liu, Y. Liu, and J. S. Bolton, "Acoustic source reconstruction and visualization based on acoustic radiation modes," *J. Sound Vib.* **437** 358-372 (2018).

[4] J. Liu, Y. Liu, and J. S. Bolton, "The application of acoustic radiation modes to engine oil pan design," SAE Technical Paper 2017-01-1844 (2017).

[5] D. M. Photiadis, "The relationship of singular value decomposition to wave-vector filtering in sound radiation problems," *J. Acoust. Soc. Am.* **88**(2) 1152-1159 (1990).

[6] G. V. Borgiotti, "The power radiated by a vibrating body in an acoustic fluid and its determination from boundary measurements," *J. Acoust. Soc. Am.* **88**(4), 1884-1893 (1990).

[7] A. Sarkissian, "Acoustic radiation from finite structures," *J. Acoust. Soc. Am.* **90**(1), 574-578 (1991).

[8] J. Liu, Y. Liu, and J. S. Bolton, "A study of the frequency and shape dependency of acoustic radiation modes," *Proc. InterNoise 2018*, Paper 1769 (2018).